The International Journal of Advanced Manufacturing Technology
https://doi.org/10.1007/s00170-025-16985-8

ORIGINAL ARTICLE

Enhancing the shear strength of adhesive bonded compression-molded CFRP laminates using selective UV picosecond laser treatment

Vincenzina Siciliani[1] · Riccardo Pelaccia[1] · Davide Castagnetti[1] · Luca Raimondi[2] · Lorenzo Donati[2] · Leonardo Orazi[1,3] · Marco Alfano[1]

Received: 1 August 2025 / Accepted: 5 November 2025

Abstract
Carbon fiber reinforced polymers (CFRP) are widely recognized for their exceptional strength-to weight ratio, making them ideal for advanced applications requiring superior mechanical performance and low weight. However, their heterogeneous composition poses challenges in both processing and surface treatment, which are crucial to improve the strength of bonded joints involving CFRP adherends. Laser processing technology offers several advantages in the processing of CFRPs, such as the effective removal of contaminants (e.g. mold release compounds) which hamper adhesion to structural adhesives. In this work, a UV picosecond laser is used to perform surface preparation of CFRP compression molding laminates. The proposed treatment not only cleans the matrix of release agents but also enables selective matrix removal without damaging the carbon fibers. Pre- and post-treatment surface morphology and chemistry are analyzed using a stereomicroscope, a digital microscope, a scanning electron microscope, and X-ray spectroscopy. The results are an improvement in the ultimate tensile strength of CFRP/CFRP single lap joints by more than 300% compared to the baseline untreated material. Furthermore, the fracture mode for laser-treated samples changes from adhesive to cohesive/fiber tearing, since the adhesive penetrates between the bare fibers.

Keywords Ultrashort laser · Ultrafast laser · Laser cleaning · Adhesive bonding · CFRP

✉ Vincenzina Siciliani
vincenzina.siciliani@unimore.it

Riccardo Pelaccia
riccardo.pelaccia@unimore.it

Davide Castagnetti
davide.castagnetti@unimore.it

Luca Raimondi
luca.raimondi@unibo.it

Lorenzo Donati
l.donati@unibo.it

Leonardo Orazi
leonardo.orazi@unimore.it

Marco Alfano
marco.alfano@unimore.it

[1] Department of Sciences and Methods for Engineering, University of Modena and Reggio Emilia, Reggio Emilia, Italy

[2] Department of Industrial Engineering, Alma Mater Studiorum Università di Bologna, Bologna, Italy

[3] EN&TECH – University of Modena and Reggio Emilia, Reggio Emilia, Italy

1 Introduction

Lightweight structural design is a cornerstone of modern transportation engineering, especially in the development of battery electric vehicles (BEVs) and hybrid electric vehicles (HEVs). Reducing vehicle mass directly improves energy efficiency and extends driving range. Carbon fiber reinforced polymers (CFRP) are increasingly used in this domain due to their high specific strength, stiffness, fatigue resistance, and low density. These materials can effectively replace metals in both secondary and primary load-bearing applications across the automotive, aerospace, and defense industries [1, 2].

Among the various composite manufacturing methods, prepreg compression molding (PCM) has emerged as a viable alternative to traditional techniques thanks to its shorter processing times, lower energy consumption, and reduced production costs, making it ideal for high-volume, cost-sensitive applications that demand consistent part quality [3]. However, integrating CFRP into main structural elements poses significant joining challenges, especially when geometric complexity or tooling constraints limit the use of monolithic designs.

Published online: 22 November 2025

In such cases, adhesive bonding is becoming the most preferred joining method, as it enables uniform load distribution, reduces stress concentrations, and preserves structural continuity without damaging the reinforcing fiber or compromising the integrity of the composite through drilling [4]. Secondary bonding with structural adhesives (i.e., adhesive bonding of cured plates) is particularly advantageous for composite assemblies, as it supports automated manufacturing processes and offers greater design flexibility.

However, the reliability of composite joints is highly dependent on surface conditions [5]. A key challenge in PCM-based composite parts stems from the use of silicone release agents on tooling surfaces. These agents often form adsorbed monolayers that can be redeposited during machining and may penetrate the initial layers of the matrix, rendering simple surface cleaning ineffective [6, 7]. Even minimal silicone contamination can severely impair bonding performance, significantly reducing joint strength and long-term durability [8, 9]. Therefore, effective surface pretreatment is essential to achieve optimal surface energy and mechanical compatibility at the adhesive–adherent interface for reliable bonding.

Because of their heterogeneous nature, CFRP composites also present significant processing challenges, including risks of delamination, extensive heat-affected zones, and fiber damage or pullout [10, 11]. In compression-molded CFRP laminates, these challenges are further exacerbated by the matrix sensitivity to thermal degradation and the irregular structure of the reinforcement fabric, complicating both conventional machining processes, as drilling or milling, and advanced surface treatment methods, as abrasive water jet machining or ultrasonic machining [10, 12].

Traditional surface preparation techniques—such as mechanical abrasion, grit blasting, and solvent-based cleaning—are commonly employed to remove surface contaminants and modify topography. However, these methods are predominantly manual, difficult to control, and pose significant challenges for integration into automated production workflows. In contrast, laser processing offers several distinct advantages for CFRP treatment, including high selectivity, precision, efficiency, and controllability, all within a non-contact framework. Laser technology is already applied to various composite operations, such as machining [13–15], cutting [16], and surface treatment [17–24], with documented improvements in bonding strength [18–21, 23]. These capabilities make laser treatments particularly attractive for scalable, automated manufacturing environments.

Laser irradiation can simultaneously remove contaminants, modify surface morphology, and enhance chemical reactivity, thereby improving both mechanical interlocking and chemical adhesion at the interface. The primary mechanisms involved in laser surface treatment include cleaning and texturing (ablation), but the overall effectiveness and outcome of laser processing of CFRP are highly dependent on key processing parameters—specifically laser mode, pulse frequency, pulse duration, and critically, the laser wavelength. Precise control over these variables is essential to achieve high-quality surface modification while minimizing thermal damage.

Laser wavelength plays a pivotal role. For example, near-infrared (NIR) lasers, which can be partially absorbed by thermoset epoxy matrices, often induce significant heat-affected zones and potential fiber degradation. Indeed, the laser ablation mechanism in CFRP when treated with near-infrared (NIR) laser radiation differs from conventional material ablation. Due to the partial transparency of epoxy to NIR wavelengths and near-total absorption of carbon fibers, the laser energy primarily causes rapid thermal degradation and vaporization of the matrix material. As noted in [25], this results in a “blasting away” effect, where the polymer matrix above carbon fibers is expelled, often leading to localized thermal damage rather than clean ablation of the composite. Nonetheless, laser-based surface treatments have shown promising results across different laser types and setups. Ultrafast IR laser texturing, for instance, has enabled damage repair by selectively removing surface resin while preserving the underlying fiber structure [19]. CO_2 laser ablation has also contributed to improved bonding performance [20], demonstrating that IR-based methods can be effective when carefully controlled. Ultrafast lasers—such as femtosecond IR pulses—have also demonstrated high effectiveness in the formation of periodic microstructures on carbon fibers, enhancing bonding performance [12].

Conversely, ultraviolet (UV) lasers offer superior beam quality and minimal thermal effects, as their shorter wavelengths are less absorbed by the polymer matrix, thereby reducing the risk of thermal damage [10]. UV laser post-treatment has been shown to leave no residue on fiber surfaces, unlike infrared (IR) lasers, which can induce swelling and form extensive heat-affected zones (HAZ). Laser-based surface treatments using UV picosecond ring-texturing [18] and incoherent UV light post-IR laser treatments [21] have significantly improved adhesion and mechanical strength compared to untreated CFRP surfaces. Notably, adhesive joints prepared with UV laser-treated surfaces have demonstrated higher average shear strength values than those with IR [26]. Furthermore, scanning strategy plays a crucial role in controlling thermal behavior: parallel scanning facilitates heat dissipation, whereas perpendicular scanning can result in localized overheating and fiber damage [12]. While aggressive laser texturing may introduce the risk of fiber damage, laser cleaning remains a promising strategy for overcoming surface preparation challenges in CFRP processing.

Despite these encouraging results, the application of laser-based surface treatments to CFRP laminates manufactured via compression molding remains relatively

underexplored, especially in addressing surface contamination caused by silicone-based release agents used in tooling. Therefore, the present study aims to fill this gap and proposes the use of a UV picosecond laser to perform surface preparation of CFRP compression molded plates. The basic objective is to clean the matrix from contaminants, such as release agents, without damaging the underlying carbon fibers. Both surface cleaning (minimum removal of surface matrix) and laser ablation (full matrix removal with exposed fibers) are analyzed to verify the impact on bonding strength. The treated CFRP specimens are adhesive bonded using a structural adhesive, and the joint strength is compared to that of the baseline bonded plates. The influence on the performance of the joint is assessed based on the average ultimate tensile strength at fracture of four specimens from a quasi-static tensile test, as well as the fracture mode, through the analysis of the fracture surfaces.

2 Materials and methods

2.1 Composite substrate and epoxy adhesive used

The substrates are manufactured from an automotive-grade prepreg (SC160/RC200P, Gurit, Newport, UK). It features a 2×2 twill weave carbon fiber fabric (Toray T300). The fabric has a nominal areal weight of 195 g/m^2, a tow size of 3 K, and is impregnated with 40% by weight of Gurit SC160 epoxy resin. The preparation of the composite material involved several distinct stages:

- Prepreg Handling.
    - ○ Extracted from cold storage and conditioned at room temperature for 5 h in a controlled white chamber environment.
- Preform Preparation.
    - ○ Cut and in square preforms measuring 320 × 320 mm in the 0° fiber direction.
    - ○ Hand lay-up performed using a stacking sequence of $[0°/90°]_6$.
- Compression Molding Process (AEM3 press):
    - ○ Mold cavity size: 320 × 320 mm.
    - ○ Tool temperature maintained at 130 °C, monitored via two thermocouples.
    - ○ Mold surface coated with Chemlease® PMR EZ release agent (Chem-Trend L.P., Howell, US).
- Post-Processing.
    - ○ Molded plates cooled in free air to ambient room temperature [27].

The mechanical properties of the cured plates, which were assessed in a previous study [28, 29], feature tensile and flexural moduli of 58 GPa and 50 GPa, respectively, with corresponding ultimate strengths of 446 MPa and 830 MPa.

Single-lap joints were fabricated following the recommendations outlined in ASTM Standard D5868 [30]. Composite panels were machined into flat coupons measuring 100 × 25 × 2.5 mm for adhesive bonding, and alignment Table (25 × 25 mm) were prepared using the same procedure.

The adhesive selected was Hysol 9466 (Henkel-Loctite), a two-component, toughened industrial grade structural epoxy well-suited for demanding service conditions where high chemical resistance and mechanical strength are required. Adhesive curing can be accomplished at room temperature for approximately 24 h, or by heating at temperatures up to 100 °C, which reduces the curing time down to 30 min. The fully cured adhesive can withstand a wide range of chemicals and solvents. The adhesive provides reliable bonding across a variety of materials, including metals and composites and is well suited for general purpose industrial applications.

2.2 UV picosecond laser treatment parameters

The entire proposed methodology is presented in Fig. 1(a). First, a picosecond laser system (Atlantic 50, Ekspla, Lithuania) with a pulse duration of approximately 10 ps was employed for surface preparation, prior to bonding and mechanical testing.

The laser system has three beamlines following the three available wavelengths − 1064 nm, 532 nm, and 355 nm-with corresponding maximum output powers of 50 W, 25 W, and 18 W, respectively. For this study, the 355 nm ultraviolet beamline was selected, as the epoxy exhibits significant absorption at this wavelength, enabling precise ablation of the composite matrix while minimizing heat conduction to the surrounding material and thereby reducing the risk of thermal damage [10, 12].

The laser operates at a repetition rate ranging from 300 kHz to 1000 kHz. Beam delivery is achieved through a galvanometric scanning head (Superscan V, Raylase, Germany) with a maximum scanning speed of 4 m/s, paired with an F-theta lens (LINOS F-Theta-Ronar Lens, Quioptiq Photonics, Germany). The beam diameter obtained is approximately 10 μm at $1/e^2$ intensity. The overall system is depicted in the schematic shown in Fig. 1(b).

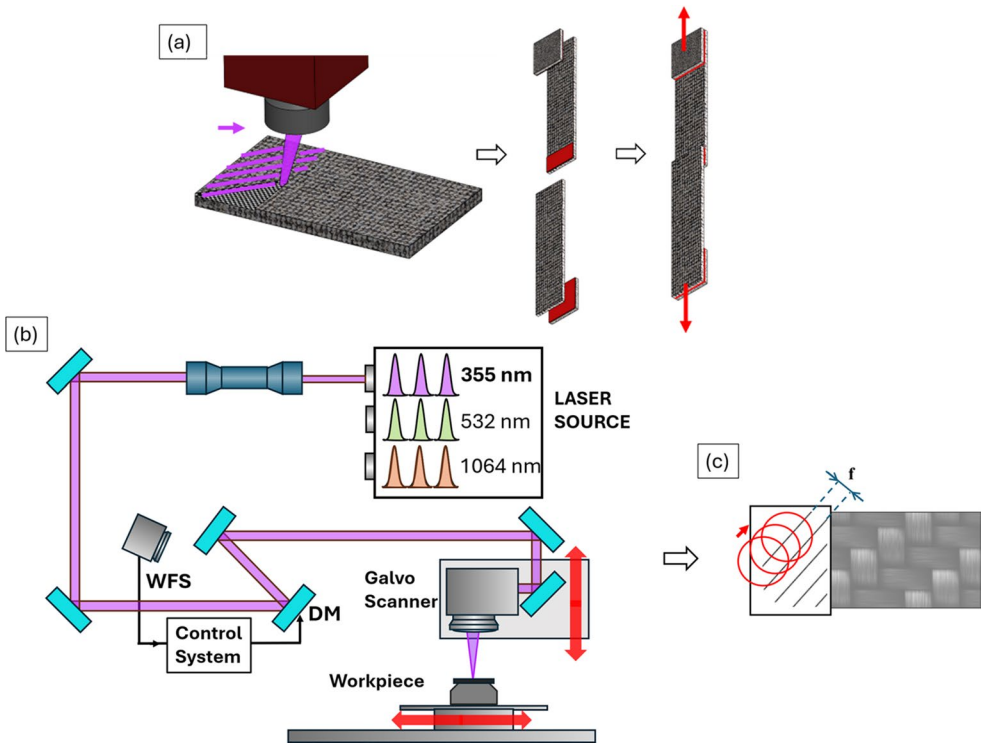

Fig. 1 (**a**) Schematic representation of the experimental methodology employed in this work; (**b**) Set-up of the multi-wavelength laser equipment; (**c**) selected scanning strategy for the laser treatment of CFRP

A preliminary study was conducted to identify suitable processing parameters, including line spacing, delivered power, and number of passes. The assessment revealed that a line spacing of 3 µm resulted in excessive heat concentration, whereas a spacing of 5 µm required higher power levels to achieve effective matrix removal. Scanning in the direction parallel to the fibers (e.g. horizontal) led to localized heat accumulation in certain regions, causing significant fiber-matrix debonding. A similar issue was observed when increasing power during a single pass. Based on these observations, the study proceeded using a qualitatively optimized set of processing parameters and adopted a progressive increase in the number of laser passes. In particular, two distinct processing strategies were investigated, namely:

- Cleaning treatment: elimination of the release agent from the surface with minimum ablation of the epoxy matrix.
- Matrix ablation: complete removal the matrix from the surface, thereby exposing the underlying carbon fibers.

To ensure uniform surface treatment, a rectangular area of 14×28 mm^2 was selected to fully encompass the adhesive bonding zone of 14×25 mm^2, thereby avoiding under-processed boundaries. The region was raster-scanned with parallel lines oriented at 45°, minimizing directional bias and avoiding preferential energy absorption by fibers aligned in horizontal or vertical directions, see Fig. 1(c). The scanning speed was set to 2000 mm/s, with a repetition rate of 600 kHz, enabling consistent energy delivery both along and between scan lines. The high frequency permitted fast scanning while maintaining sufficient energy per pulse, as supported by the laser source.

The final values of the laser parameters were as follows: 4 µm-spaced parallel lines at a 45° orientation ("f" in Fig. 1(c)), scanning speed 2000 mm/s, repetition rate of 600 kHz, and an average laser power of 1.5 W. This corresponds to a pulse energy of 2.5 µJ and a fluence rounding at 3.2 J/cm^2 per pass. To achieve the desired surface modification, the number of laser passes was tailored: eight passes were used for laser cleaning, while laser ablation was accomplished with approximately thirty passes.

After laser processing, the treated surfaces were cleaned with isopropyl alcohol to remove any residual dust or debris that could interfere with adhesive bonding. The same degreasing procedure was applied to the samples not subjected to laser treatment, ensuring identical baseline conditions for all specimens.

2.3 Single-lap joint manufacturing and mechanical testing

Following laser treatment, CFRP surfaces were cleaned, and a layer of adhesive was applied to the bonding region of the bottom adherend. To ensure constant bondline

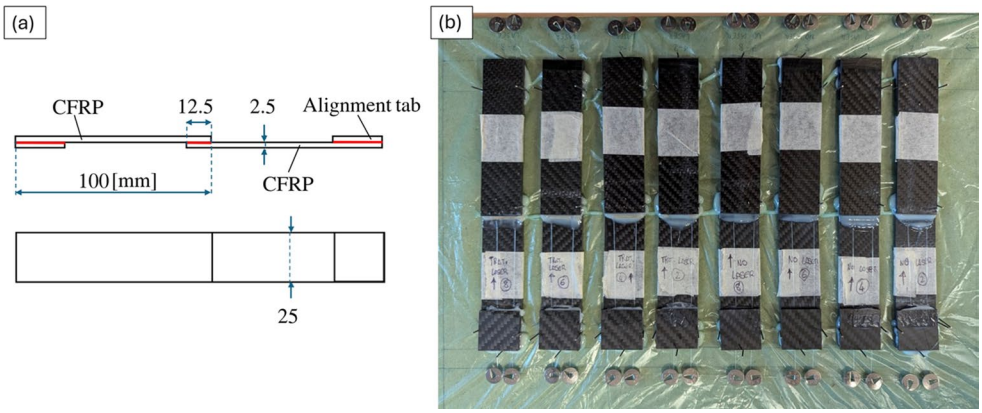

Fig. 2 (**a**) Dimensions of the specimens and the bonded area; (**b**) actual bonded specimens

thickness, two evenly spaced nylon wires (260 µm-thick) were positioned along the bonding area and parallel to the loading direction, serving as spacers. After adhesive application, the top adherend was accurately positioned using a custom-designed fixture to ensure proper joint alignment. Alignment tabs were then bonded following the same procedure. Figure 2 shows a schematic representation of the assembled single-lap joint (a), along with a top-view image of actual fabricated joints (b). The schematic highlights key geometric features, including the adherend dimensions, bonded overlap length, and the adhesive layer thickness.

As recommended by the adhesive manufacturer technical data sheet, the joints were clamped to hold the assembly in place and to squeeze out the excess adhesive. Curing was carried out at 40 °C for 3 h to achieve satisfactory mechanical properties.

Following curing, all specimens were inspected to confirm consistency in joint alignment, bondline integrity, and overall manufacturing quality.

Mechanical testing was performed using an electromechanical tensile testing machine (Quasar 25, Galdabini, Italy) equipped with a 25 kN loading cell. Each specimen was carefully aligned with the loading axis and secured in the grips. A preload of 200 N was applied, followed by a constant displacement rate of 1 mm/min until failure. Force-displacement curves were recorded for each test.

For each laser treatment condition, four single-lap adhesive joint specimens were prepared and tested to evaluate the mechanical properties.

2.4 Characterization of surface morphology and chemistry

To gain an overview of the samples pre- and post-laser processing, a stereoscope (Stemi 2000 C, Zeiss, Germany) equipped with 5 objectives (0.65-5x) and a digital microscope (VHX, Keyence, Japan) equipped with 2 optical objectives (100-500x and 500-2500x) was used for initial surface inspection.

For more detailed surface characterization, a scanning electron microscope (Nova NanoSEM 450, Fei, Oregon) was used to examine the surface morphology of the specimens at various magnifications. Surface composition analysis was conducted using an energy dispersive spectroscopy system (X-EDS Oxford INCA-350, Oxford Instrument, England) integrated with the SEM.

Global EDS spectra were acquired by averaging the signal over a 120-second acquisition period. Elemental mapping was carried out with an integration of 5 min per area, performed on both untreated and laser-treated specimens. Data were collected from three distinct regions on each sample, with each measuring approximately 140 × 105 µm.

3 Results and discussion

3.1 Stereoscopy and SEM microscopy morphological results

A comparison between untreated and laser-treated surfaces, as observed under the stereoscope, is presented in Fig. 3.

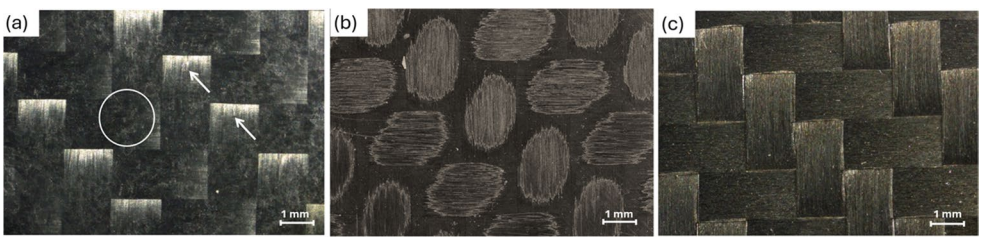

Fig. 3 Stereoscopic images of CFRP surfaces: (**a**) untreated, (**b**) laser cleaned, and (**c**) laser ablated

Corresponding higher magnification images acquired with the digital microscope are shown in Fig. 4.

The untreated material in Fig. 3(a) and Fig. 4(a) and (d) exhibits white patches scattered across the surface (one example is highlighted by a circle). Thicker regions of the epoxy matrix are evident through localized light reflections (indicated by white arrows), due to the smoother and more transparent nature of the resin, which reflects light more efficiently under oblique illumination. These resin-rich areas produce distinct bright spots. In contrast, the darker areas correspond to carbon fiber bundles that are positioned closer to the surface. These fibers absorb more light and exhibit less surface reflectivity, resulting in a matte or shadowed appearance. This optical contrast is particularly pronounced in 2×2 twill weave fabrics, where the regular undulating pattern leads to alternating regions of resin accumulation and near-surface fiber exposure.

In the cleaning treatment condition - Fig. 3(b) and Fig. 4(b, e) - the surface appears more uniform, with the larger stains noticeably reduced. Fiber bundles begin to emerge more distinctly, and although laser tracks are visible on the matrix, there are no apparent signs of burning or damage. The matrix retains its semi-transparent appearance, suggesting limited thermal degradation.

In contrast, the matrix ablation condition - Fig. 3(c), Fig. 4(c, f) - shows that the semi-transparent epoxy matrix has been almost entirely removed. As a result, the underlying woven carbon fiber bundles are clearly exposed across the treated surface. The two types of treatment also differ in the average extent of treatment depth. For the case of ablation compared to cleaning, they increase more than twice as much (from about 40 µm to about 100 µm), at points where the fiber bundle is further from the surface.

After laser treatment, the carbon fibers appear largely intact and free from visible damage. As shown in Fig. 5 (a) and (b), when the laser passes directly over exposed fibers following complete matrix removal, a gentle interaction characteristic of ultra-short pulse lasers is observed. This interaction leads to the formation of Laser Induced Periodic Surface Structures (LIPSS) [31], which are submicrometer features typically measuring around 100 nm. These nanostructures form on the fiber surfaces, also where the fiber tows change direction and break continuity, effectively restoring some degree of surface uniformity. LIPSS are known to orient perpendicular to the laser polarization plane [31], which results in the alignment with certain fiber bundles and perpendicularly with others.

These surface modifications can influence the behavior of the fibers prior to re-impregnation with epoxy resin, potentially enhancing interfacial bonding and improving the mechanical performance of the composite. In the context of adhesive bonding, such nanostructuring may increase adhesion at the fiber-adhesive interface. Notably, in a recent

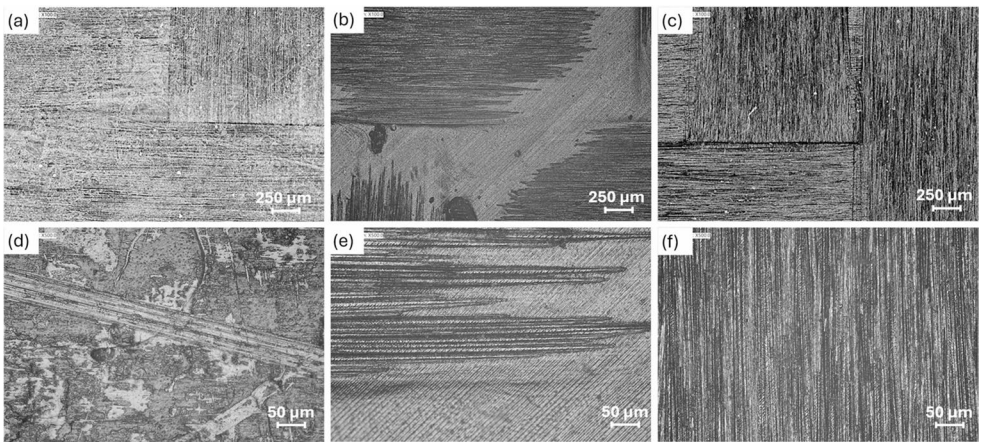

Fig. 4 Digital microscope images at different magnifications: (**a**), (**d**) untreated; (**b**), (**e**) laser cleaned and (**c**), (**f**) laser ablated

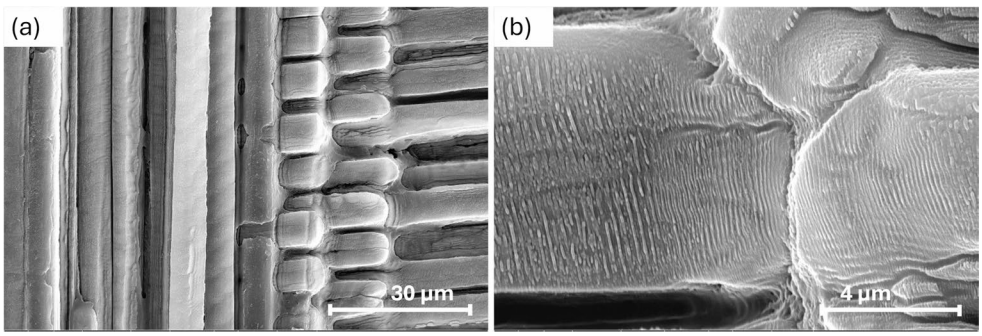

Fig. 5 SEM images highlighting the LIPSS structures obtained on the fibers' surface at different magnifications: (**a**) 4000x, (**b**) 30000x

review in the area of composite joints [32], it was pointed out that interlaminar strength and toughness can be significantly improved through nano-engineered interfacial layers, which leads us to surmise that similar benefits may be achieved through the presence of LIPSS.

3.2 EDX spectroscopy chemical results

Analysis of the surface chemistry before and after laser treatment reveals a notable change in elemental composition. In the EDS spectra of Fig. 6(a), the characteristic silicon peak—attributed to the silicone-based release agent that permeated the matrix during the compression molding process—is clearly visible in the untreated material but disappears following both laser treatments. The spectra for the two laser-treated conditions (dashed and dotted lines) appear almost completely overlapping, indicating similar chemical outcomes regardless of the specific laser processing strategy. Despite this, the differences between the two treatments are evident in the microscope images shown in the previous section.

In the analysis, the other elements attributable mainly to the matrix were neglected, which are not significant for the objective of evaluating the removal of the release agent. In particular, quantitative elemental analysis performed via EDS confirms a significant redistribution of surface elements following laser treatment: all laser-treated samples exhibit a marked reduction in silicon content, accompanied by a relative increase in carbon concentration. This trend is consistent with the removal of the silicone-based release agent and partial or complete ablation of the epoxy matrix.

To ensure representative data, mass percentage measurements were collected from three distinct surface regions for each treatment condition - see Fig. 6(b). In the untreated material, the silicon content demonstrates considerable variability, as indicated by the large standard deviation and corresponding error bars in the histogram. This heterogeneity can be attributed to two main factors: first, the localized accumulation of the release agent in discrete patches during compression molding, and second, the uneven distribution and thickness of the epoxy matrix over the woven carbon fibers. Thicker areas of matrix material tend to retain more of the contaminant, while thinner regions may expose fiber bundles more directly, resulting in inconsistent silicon detection.

In contrast, the laser-treated surfaces exhibit not only reduced silicon levels but also significantly lower variability across sampling locations, suggesting that the laser treatment—whether aimed at cleaning or matrix ablation—effectively homogenizes the surface composition. This uniformity is particularly important in applications involving adhesive bonding, where surface chemistry consistency strongly influences joint performance and reliability [33].

Figure 7(a)-(c) present SEM and EDS images of untreated composite samples, while Fig. 8(a)-(c) show the corresponding images for the laser treated samples: (a), (b) cleaning; (c) ablation. In the EDS elemental maps, carbon is indicated in black and silicon in white.

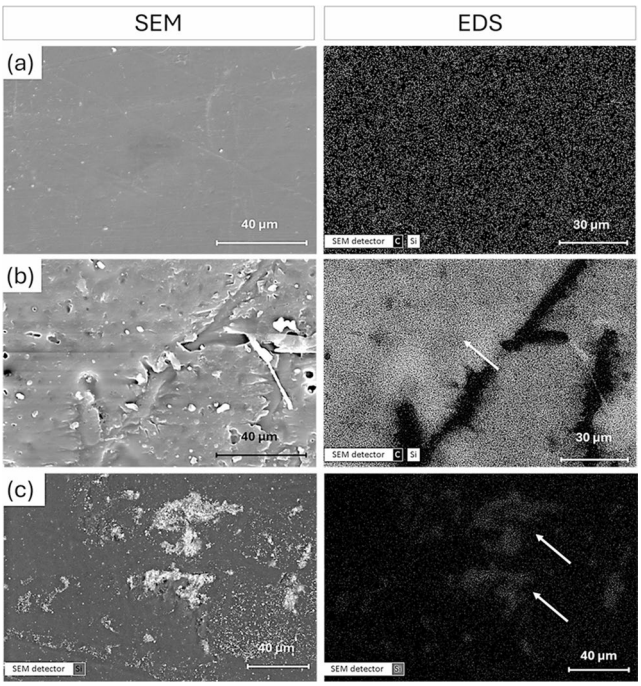

Fig. 7 SEM images and EDS elemental map of untreated CFRP surfaces: three different analysed zones in (**a**), (**b**), (**c**)

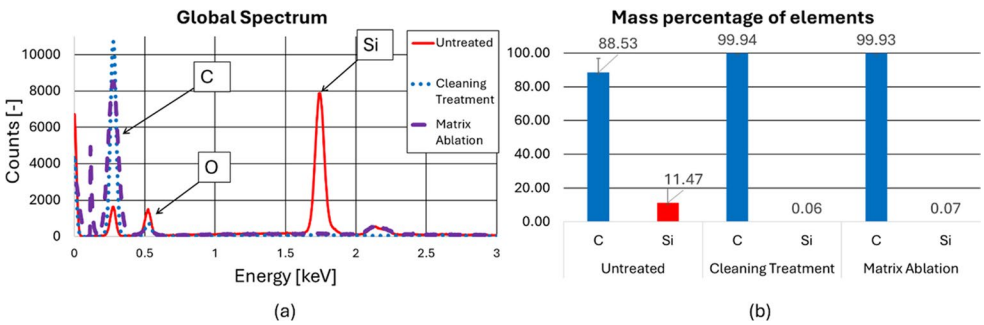

Fig. 6 EDS spectroscopy analysis of untreated and laser treated surfaces: (**a**) global spectrum; (**b**) mass percentage of silicon and carbon

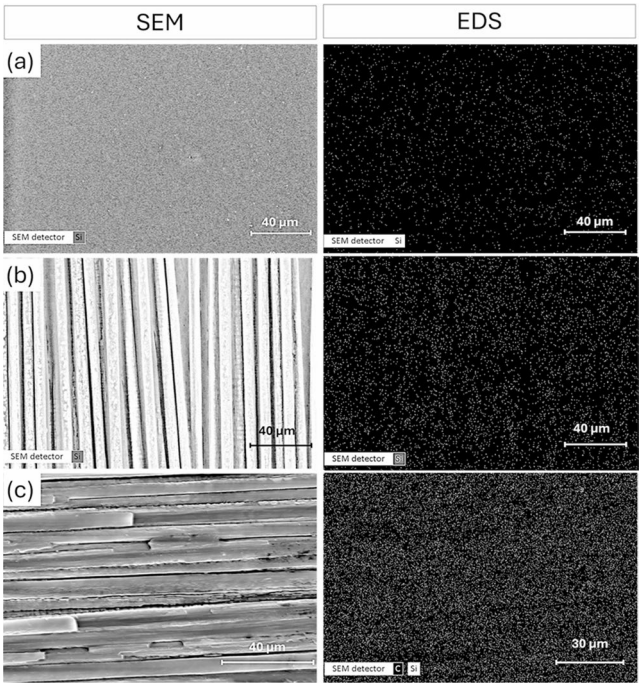

Fig. 8 SEM images and EDS elemental map of laser treated surfaces: (**a**) matrix and (**b**) fibers in cleaning treatment; (**c**) are fibers in the ablation treatment

From the morphological analysis of the untreated samples, Fig. 7(a)-(c), it is confirmed that the three examined zones differ significantly from one another. The micrographs reveal clusters of silicon-rich regions, predominantly in the form of agglomerated white dots. These are attributed to the presence of the release agent, as highlighted by the white arrows in the images.

Following the laser cleaning treatment, notable changes are observed. In the polymer matrix region, Fig. 8(a), silicon dots are still present, but they appear much more sparsely distributed compared to the untreated condition. Additionally, no significant variations are observed between different locations within the matrix, indicating a homogenizing effect of the laser treatment.

At the level of the fiber region in the cleaning treatment, Fig. 8(b), no detectable silicon is observed (i.e., a silicon content of approximately 0%), suggesting that the laser effectively removed the release agent for the fiber surfaces. This observation is consistent with the results from the matrix ablation, Fig. 8(c), where silicon is also absent across all analyzed zones.

Overall, in the laser-treated samples, the elemental distribution is more uniform and consistent across various regions, with only minor local variations. This supports the conclusion that the laser treatment effectively removes surface contaminants, particularly silicon-based residues, and produces a more chemically homogeneous surface.

3.3 Mechanical test results

Single lap shear tests were conducted on three batches, each comprising four specimens. A comparison between the untreated joints and the two laser-treated conditions demonstrates the effectiveness of laser surface treatment. Figure 9 presents the tensile test results (a) and average shear strength values (b); for clarity, only one representative force-displacement curve is shown per batch.

The cleaning laser treatment resulted in a 252% increase in average shear strength, while the matrix ablation treatment led to a further 14.5% improvement, reaching a total enhancement of 303% over the untreated condition (Table 1). This corresponds to a rise in average shear strength from 4.76 MPa to 19.2 MPa. The laser treatment also contributed to a notable increase in displacement at break, which likely due to the moderate increase of the peak load across the experiments. Overall, the consistency of results across

Table 1 Breakdown of the single lap joint test results

	Untreated	Cleaning Treatment	Matrix Ablation
[MPa]	4.76±0.41	16.77±1.91	19.2±3.24
[%]	-	+252	+303

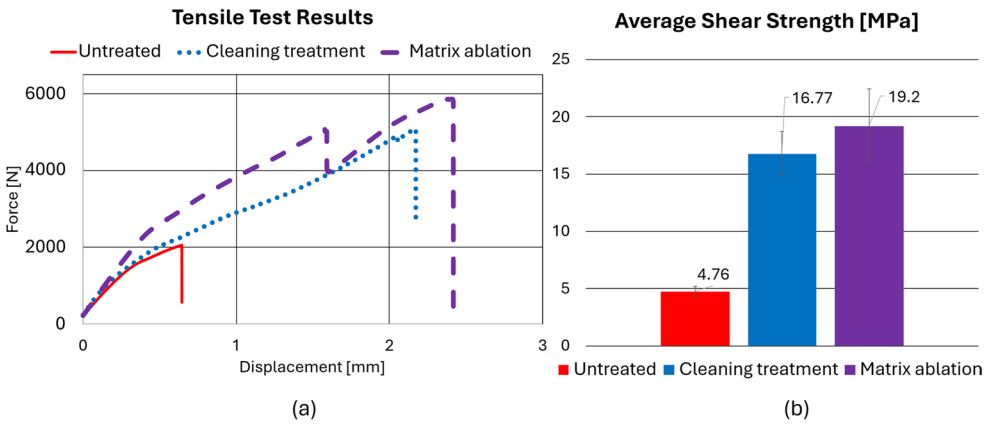

Fig. 9 (**a**) Representative load-displacement plots obtained in tensile tests; (**b**) average shear strength of the single lap joints

samples confirms the reproducibility and reliability of the laser treatment strategy.

The mechanical improvement aligns with the SEM and EDS observations, which confirmed a significant reduction in surface contaminants, particularly the silicon-based residues originating from the release agent. In the untreated samples, EDS mapping revealed widespread silicon agglomerates on both the fiber and matrix surfaces that, as stated earlier, are known to interfere with adhesive bonding. Conversely, laser-treated samples exhibited a cleaner substrate, with minimal or no silicon detected, especially in the matrix ablation condition.

Besides, we attribute the improvement of joint strength for laser treated samples primarily to the removal of the top-most polymer matrix layer, that enables the adhesive to bond directly to the carbon fibers. As discussed earlier, the polymer matrix often retains surface contaminants that hinder adhesion to epoxy. Although EDS spectra for both cleaning and ablation treatments appear quite similar, this technique has limited depth sensitivity and may not detect subtle differences in surface contamination, especially if contaminants are embedded within the matrix. By eliminating the matrix layer, the bonding interface becomes more conducive to strong adhesion.

In addition to contaminant removal, the proposed laser ablation treatment exposes a greater portion of the fiber surface compared to the cleaning treatment. This increased exposure likely enhances chemical interaction with the adhesive and may contribute to higher surface energy. Furthermore, as shown in Fig. 5, the laser ablation process induces a texture on the carbon fiber surface, which is deemed to increase available surface area and promote mechanical interlocking sites.

Collectively, contaminant removal, increased fiber exposure, higher surface energy, and enhanced mechanical interlocking, can explain the substantial improvement in joint strength observed with matrix ablation, with increases up to 300%.

3.4 Analysis of fracture surfaces

Fractographic analysis of the untreated joints using stereomicroscopy reveals a predominantly adhesive failure mode. As shown in Fig. 10(a) and Fig. 10(d), the adhesive is seen to remain almost entirely on one adherend, while completely detaching from the mating surface - indicative of limited interfacial bonding. Several regions exhibit poor wetting behavior, where the adhesive fails to uniformly spread, leading to the formation of voids or air pockets as shown in Fig. 10(b) and (e). At higher magnification, Fig. 10 (c) and (f), the surfaces do not exhibit any distinctive morphological features associated with cohesive failures. The absence of such features, along with the presence of unbonded zones and surface separation, suggests that surface contamination or lack of surface preparation may have contributed to poor adhesion and weak mechanical response.

In contrast, the cleaning treatment led to noticeably improved adhesion, as indicated by fiber pull-out from the adherend and the presence of adhesive residues on both fracture surfaces, see Fig. 11(a) and (d). Although the fracture does not correspond to a classic cohesive failure, enhanced adhesion appears to increase resistance to interfacial separation. Consequently, the crack path in some regions transitions from the upper to the lower near-interfacial region, and vice versa, leaving adhesive residue on both sides. The stereoscopic images and the tilted SEM view in Fig. 11(c), which shows the adhesive pulling out fibers from the adherend, further supports this interpretation.

Indeed, the fracture surface images under matrix ablation conditions reveal a significant increase in adhesion where the fibers remained exposed. In addition to the observed fiber tearing, clearly visible in Fig. 12(a) and (b), regions where the adhesive remained on the surface exhibit micrometric-level replication of the fibers. Specifically, Fig. 12(c) shows the exposed fibers, while Fig. 12(f) illustrates the corresponding fiber shape replicated on the adhesive.

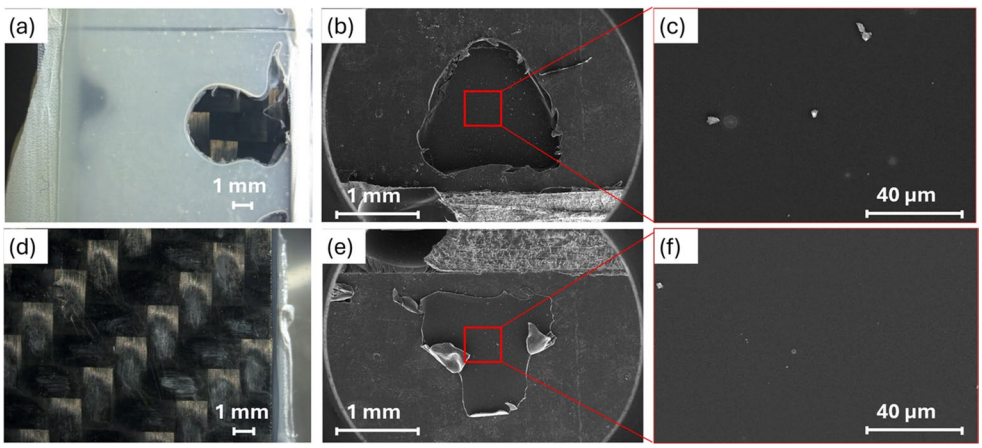

Fig. 10 Fracture surfaces of untreated specimens: (**a**) stereoscope images of the top adherend; (**b**) SEM analysis at a void location; (**c**) magnified view of the region inside the void. (**d**) Stereoscope image of the bottom adherend; (**e**) SEM analysis of the adhesive residual on the bottom adherend; (**f**) magnified view of the top surface of the adhesive residual shown in (**e**)

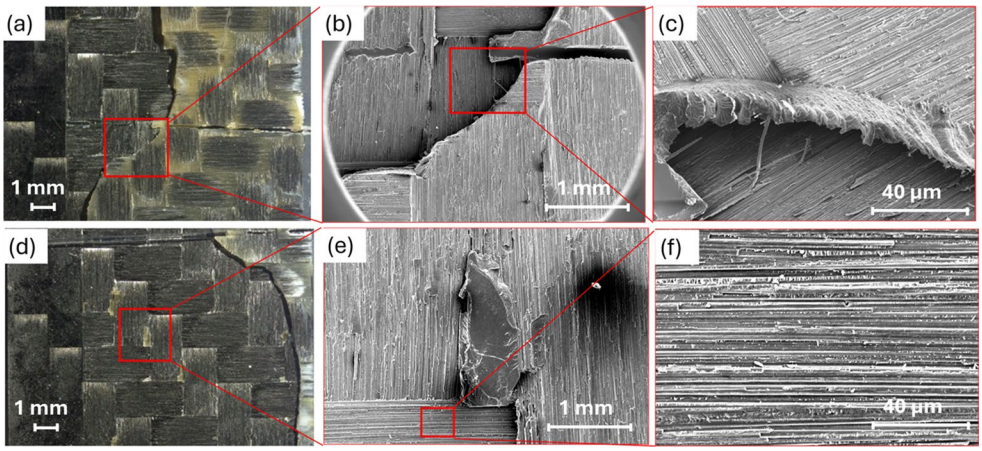

Fig. 11 Fracture surfaces of cleaned specimens: (**a**) stereoscope images of the top adherend; (**b**) SEM images of fiber pulled from the adhesive in 2D; (**c**) magnified and tilted 3D view. (**d**) Stereoscope images of the bottom adherend; (**e**) detail of adhesive interposed between the fiber bundles; (**f**) adhesive particles adhered to the surface of the composite fibers

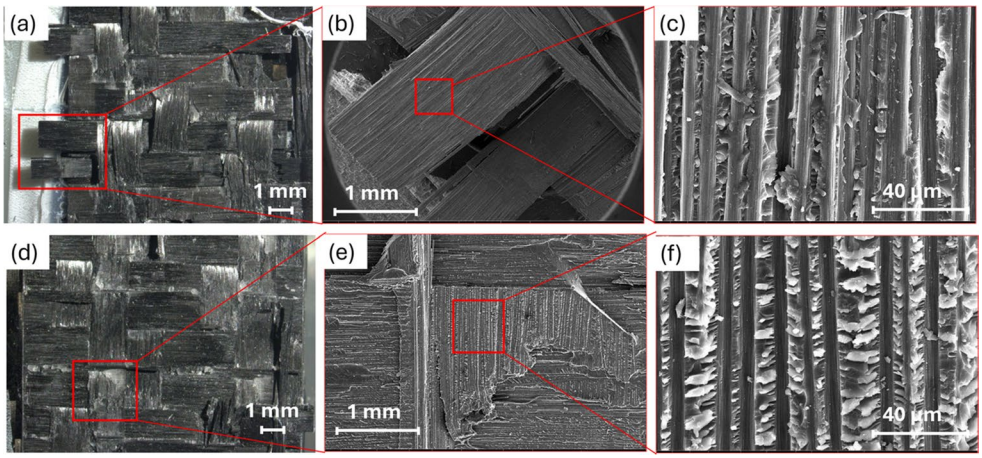

Fig. 12 Matrix ablation treatment surface fracture: (**a**) stereoscope images of top adherend; (**b**) SEM images of pulled fiber bundle after tensile test in a tilted view; (**c**) magnified view of the fibers in a 2D view. (**d**) Stereoscope images of bottom adherend; (**e**) detail of adhesive interposed between the fiber bundles; (**f**) replication of the fiber shape at the micrometric level

It is worth noting that the absence of fully cohesive failure is attributed to the relatively higher strength of the selected epoxy adhesive compared to the mechanically weaker near-surface region of the treated laminates, which remains the limiting factor in the joint performance.

4 Conclusions

This study explored the use of a 355 nm picosecond ultraviolet (UV) laser for selective surface treatment of CFRP composites manufactured via the Prepreg Compression Molding (PCM) process. The objective was to remove surface contaminants, which are primarily release agents, without damaging the underlying fibers. Two treatment strategies were assessed: one focused on matrix cleaning, and the other on localized removal of the matrix to expose carbon fibers.

Laser treatment led to a significant enhancement in joint performance, with increases in ultimate tensile strength of up to 303% compared to untreated surfaces. The observed transition in fracture behavior—from predominantly adhesive to mixed cohesive and fiber-tearing modes—indicates improved adhesion. However, the performance of the joint is limited by the relatively higher strength of the selected epoxy adhesive compared to the laminate.

The improvements can be attributed to two key effects: the effective removal of contaminants that inhibit adhesion, as confirmed by elemental and quantitative EDS analysis; and the modification of surface topography, particularly through partial fiber exposure, which enhances mechanical interlocking and contributes to increased bond strength.

The results substantiate the practicality and potential novelty of using picosecond UV-laser surface treatments for enhancing the bond quality of compression molded CFRP plates—a manufacturing route particularly susceptible to release agent contamination. Unlike traditional surface treatments, laser enables precise and selective removal of the resin matrix or surface contaminants without mechanical damage to the fibers. The formation of laser-induced periodic surface structures (LIPSS) on exposed fibers introduces an additional degree of surface functionalization at the micro- and nanoscale. These structures, which can be actively tailored using polarization optics, offer new opportunities to improve both interlaminar and adhesive bond performance, and represent a promising area for further optimization in advanced composite joining technologies.

Acknowledgements This work was supported by PNRR–M4C2INV1.5, NextGenerationEU-Avviso 3277/2021 -ECS_00000033-ECOSISTER-spk 3.
The authors wish to thank Eng. Simone Zanetti at Henkel Italia S.r.l., Milano, Italy, for supplying the epoxy adhesive employed in this research.

Funding Open access funding provided by Università degli Studi di Modena e Reggio Emilia within the CRUI-CARE Agreement.

Declarations

This work was supported by PNRR–M4C2INV1.5, NextGeneration-EU-Avviso 3277/2021 -ECS_00000033-ECOSISTER-spk 3.

Competing interest The authors have no relevant financial or non-financial interests to disclose.

References

1. Cocchi D, Raimondi L, Brugo TM, Zucchelli A (2020) A systematic material-oriented design approach for lightweight components and the CFRP motor wheel case study. Int J Adv Manuf Technol 109:2133–2153. https://doi.org/10.1007/s00170-020-05756-2
2. Falaschetti MP, Semprucci F, Birnie Hernández J, Troiani E (2025) Experimental and numerical assessment of crashworthiness properties of composite materials: a review. Aerosp 12(2):122. https://doi.org/10.3390/aerospace12020122
3. Lunetto V, Galati M, Settineri L, Iuliano L (2023) Sustainability in the manufacturing of composite materials: a literature review and directions for future research. J Manuf Process 85:858–874. https://doi.org/10.1016/j.jmapro.2022.12.020
4. Progress in adhesive-bonded composite joints: A comprehensive review - N. Karthikeyan, Jesuarockiam Naveen (2024) (n.d.). https://journals.sagepub.com/doi/10.1177/07316844241248236 (accessed July 17, 2025)
5. Morano C, Tao R, Alfano M, Lubineau G (2021) Effect of mechanical pretreatments on damage mechanisms and fracture toughness in CFRP/Epoxy joints. Materials 14:1512. https://doi.org/10.3390/ma14061512
6. Schmid Fuertes TA, Kruse T, Körwien T, Geistbeck M (2015) Bonding of CFRP primary aerospace structures – discussion of the certification boundary conditions and related technology fields addressing the needs for development. Compos Interfaces 22:795–808. https://doi.org/10.1080/09276440.2015.1077048
7. Ledesma R, Palmieri F, Connell J, Yost W, Fitz-Gerald J (2018) Surface characterization of carbon fiber reinforced polymers by picosecond laser induced breakdown spectroscopy. Spectrochim Acta B At Spectrosc 140:5–12. https://doi.org/10.1016/j.sab.2017.11.014
8. Ledesma RI, Palmieri FL, Lin Y, Belcher MA, Ferriell DR, Thomas SK, Connell JW (2020) Picosecond laser surface treatment and analysis of thermoplastic composites for structural adhesive bonding. Compos Part B Eng 191:107939. https://doi.org/10.1016/j.compositesb.2020.107939
9. Tao R, Alfano M, Lubineau G (2018) Laser-based surface patterning of composite plates for improved secondary adhesive bonding. Compos Part A Appl Sci Manuf 109:84–94. https://doi.org/10.1016/j.compositesa.2018.02.041
10. Zuo P, Liu T, Li F, Wang G, Zhang K, Li X, Han W, Tian H, Zhu D (2025) Research progress on laser processing of carbon fiber composite materials. Polym Compos 46:4992–5017. https://doi.org/10.1002/pc.29287
11. Zheng Z, Wu C, Yu X, Wang Z, Ma Y (2024) Research progress on laser processing of carbon fiber-reinforced composites. Int J Adv Manuf Technol 134:4041–4069. https://doi.org/10.1007/s00170-024-14374-1
12. Gu J, Su X, Jin Y, Zhang D, Li W, Xu J, Guo B (2024) Research progress and prospects of laser cleaning for CFRP: a review. Compos Part A Appl Sci Manuf 185:108349. https://doi.org/10.1016/j.compositesa.2024.108349
13. Lima MSF, Sakamoto JMS, Simoes JGA, Riva R (2013) Laser processing of carbon fiber reinforced polymer composite for optical fiber guidelines. Phys Procedia 41:572–580. https://doi.org/10.1016/j.phpro.2013.03.118
14. Wolynski A, Herrmann T, Mucha P, Haloui H, L'huillier J (2011) Laser ablation of CFRP using picosecond laser pulses at different wavelengths from UV to IR. Phys Procedia 12:292–301. https://doi.org/10.1016/j.phpro.2011.03.136
15. Canel T, Kayahan E, Fidan S, Sinmazcelik T (2021) Laser process parameter optimization of dimple created on oriented carbon fiber reinforced epoxy composites. J Compos Mater 55:4029–4043. https://doi.org/10.1177/00219983211031629
16. Freitag C, Wiedenmann M, Negel J-P, Loescher A, Onuseit V, Weber R, Abdou Ahmed M, Graf T (2015) High-quality processing of CFRP with a 1.1-kW picosecond laser. Appl Phys A 119:1237–1243. https://doi.org/10.1007/s00339-015-9159-3
17. Li K, Lu J, Deng Y, Xu J, Sun S, Hu J (2025) Mechanism of selective texturing of CFRP by femtosecond laser. Compos Part B Eng 291:112000. https://doi.org/10.1016/j.compositesb.2024.112000
18. Zhao C, Yan W, Sun J, Zhao F, Ma Z, Lei J (2025) Enhancing shear strength of adhesive joint of high modulus CFRP with UV picosecond laser texturing technique. Compos Struct 365:119190. https://doi.org/10.1016/j.compstruct.2025.119190
19. Shu S, He Y, Li W, He W, Zhou L, Pan X, Xuan S, Rong Y, Chen L, Jin G (2025) A high bonding tensile strength of CFRP ultrafast laser surface texturing method for surface damage repair. Opt Laser Technol 180:111601. https://doi.org/10.1016/j.optlastec.2024.111601
20. Sorrentino L, Marfia S, Parodo G, Sacco E (2020) Laser treatment surface: an innovative method to increase the adhesive bonding of ENF joints in CFRP. Compos Struct 233:111638. https://doi.org/10.1016/j.compstruct.2019.111638
21. Al-Mahdy A, Ahuir-Torres JI, Öpöz TT, Kotadia HR, Mullett J, Sharp MC (2025) An investigation into the use of incoherent UV light to augment IR nanosecond pulsed laser texturing of CFRP composites for improved adhesion. Opt Laser Technol 181:111626. https://doi.org/10.1016/j.optlastec.2024.111626
22. Piscitelli F, De Palo R, Volpe A (2023) Enhancing coating adhesion on fibre-reinforced composite by femtosecond laser texturing. Coatings 13:928. https://doi.org/10.3390/coatings13050928
23. Sorrentino L, Parodo G, Turchetta S (2022) Influence of laser treatment on end notched flexure bonded joints in carbon fiber

reinforced polymer: experimental and numerical results. Materials 15:910. https://doi.org/10.3390/ma15030910
24. Liu Z, Cheetham S, Dilworth S, Li L (2014) Laser abrading of carbon fibre reinforced composite for improving paint adhesion. Appl Phys A 117:1045–1054. https://doi.org/10.1007/s00339-014-8527-8
25. Fischer F, Kreling S, Jäschke P, Frauenhofer M, Kracht D, Dilger K (2012) Laser surface pre-treatment of CFRP for adhesive bonding in consideration of the absorption behaviour. J Adhes 88:350–363. https://doi.org/10.1080/00218464.2012.660042
26. Li Y, Zhan X, Gao C, Wang H, Yang Y (2019) Comparative study of infrared laser surface treatment and ultraviolet laser surface treatment of CFRP laminates. Int J Adv Manuf Technol 102:4059–4071. https://doi.org/10.1007/s00170-019-03368-z
27. Siciliani V (2025) Effect of surface Preparation on adhesive bonding of CFRP compression molding laminates. 2193–2202. https://doi.org/10.21741/9781644903599-236
28. Raimondi L, Brugo TM, Zucchelli A (2021) Fiber misalignment analysis in PCM-UD composite materials by full field nodal method. Compos Part C: Open Access 5:100151. https://doi.org/10.1016/j.jcomc.2021.100151
29. Raimondi L (2024) Effects of UD and twill reinforcements in hybrid sheet molding compound laminates. Mater Res Proc. https://doi.org/10.21741/9781644903131-58
30. Standard Test Method for Lap Shear Adhesion for Fiber Reinforced Plastic (2025) (FRP) Bonding, (n.d.). https://store.astm.org/d5868-01r14.html
31. Orazi L, Romoli L, Schmidt M, Li L (2021) Ultrafast laser manufacturing: from physics to industrial applications. CIRP Ann 70:543–566. https://doi.org/10.1016/j.cirp.2021.05.007
32. Lubineau G, Alfano M, Tao R, Wagih A, Yudhanto A, Li X, Almuhammadi K, Hashem M, Hu P, Mahmoud HA, Oz F (2024) Harnessing extrinsic dissipation to enhance the toughness of composites and composite joints: a state-of-the-art review of recent advances. Adv Mater 36:2407132. https://doi.org/10.1002/adma.202407132
33. Yudhanto A, Alfano M, Lubineau G (2021) Surface preparation strategies in secondary bonded thermoset-based composite materials: a review. Compos Part A Appl Sci Manuf 147:106443. https://doi.org/10.1016/j.compositesa.2021.106443